Published in final edited form as:

FASEB J. 2020 November ; 34(11): 15252–15268. doi:10.1096/fj.202001104R.

Maternal and fetal alkaline ceramidase 2 is required for placental vascular integrity in mice

Fang Li[#1,2,3], **Ruijuan Xu**[#1,2], **Chih-Li Lin**[1,2], **Benjamin E. Low**[4], **Louise Cai**[2], **Sally Li**[2], **Ping Ji**[1], **Liqun Huang**[1], **Michael V. Wiles**[4], **Yusuf A. Hannun**[1,2], **Lina M. Obeid**[1,2,5], **Ye Chen**[3], **Cungui Mao**[1,2]

[1]Department of Medicine and Cancer Center at State University of New York at Stony Brook, NY 11794, USA

[2]Cancer Center at State University of New York at Stony Brook, NY 11794, USA

[3]Guangdong Provincial Key Laboratory of Gastroenterology, Department of Gastroenterology, Nanfang Hospital, Southern Medical University, Guangzhou, Guangdong Province 510515, China

[4]Technology Evaluation and Development, The Jackson Laboratory, Bar Harbor, Maine, USA

[5]Ralph H. Johnson Veterans Administration Hospital, Stony Brook, New York, USA

[#] These authors contributed equally to this work.

Abstract

Sphingolipids have been implicated in mammalian placental development and function, but their regulation in the placenta remains unclear. Herein we report that alkaline ceramidase 2 (ACER2) plays a key role in sustaining the integrity of the placental vasculature by regulating the homeostasis of sphingolipids in mice. The mouse alkaline ceramidase 2 gene (*Acer2*) is highly expressed in the placenta between embryonic day (E) 9.5 and E12.5. *Acer2* deficiency in both the mother and fetus decreases the placental levels of sphingolipids, including sphingoid bases (sphingosine and dihydrosphingosine) and sphingoid base-1-phosphates (sphingosine-1-phophate and dihydrosphingosine-1-phosphate) and results in the *in utero* death of ≈ 50% of embryos at E12.5 whereas *Acer2* deficiency in either the mother or fetus has no such effects. *Acer2* deficiency causes hemorrhages from the maternal vasculature in the junctional and/or labyrinthine zones in E12.5 placentas. Moreover, hemorrhagic but not non-hemorrhagic *Acer2*-deficient placentas exhibit an expansion of parietal trophoblast giant cells with a concomitant decrease in the area of the fetal blood vessel network in the labyrinthine zone, suggesting that *Acer2* deficiency results in embryonic lethality due to the atrophy of the fetal blood vessel network in the placenta. Taken

Address correspondence to: Cungui Mao, PhD, Department of Medicine, 9M0834, MART Building, Stony Brook University, Stony Brook, NY 11794, USA; Tel. 001-(631)216-2904; and cungui.mao@stonybrook.edu., Ye Chen, MD, PhD, State Key Laboratory of Organ Failure Research, Guangdong Provincial Key Laboratory of Gastroenterology, Department of Gastroenterology, Nanfang Hospital, Southern Medical University, 1838 North Guangzhou Road, Guangzhou, 510515, China. Tel. 086-(139)2229-3223; yechen@smu.edu.cn.

AUTHOR CONTRIBUTIONS

F. Li, R.Xu, Y. Chen, and C. Mao designed research studies; F. Li, R. Xu, C. Lin, B. Low, L. Cai, S. Li, P. Ji, L. Huang, and M. Wiles conducted experiments; F. Li and R. Xu acquired data; F. Li, R.Xu, and C. Mao analyzed data; L.M. Obeid and Y.A. Hannun assisted research designs; F. Li, Y. Chen, and C. Mao wrote the manuscript.

This work is dedicated to the memory of Professor Lina M. Obeid

together, these results suggest that ACER2 sustains the integrity of the placental vasculature by controlling the homeostasis of sphingolipids in mice.

Keywords

ACER2; ceramidase; placenta; sphingosine; sphingosine-1-phosphate; vasculature

INTRODUCTION

The rodent or human placenta contains cells of both fetal and maternal origin and can be divided into three distinct zones: the decidual zone (DZ), junctional zone (JZ), and labyrinthine zone (LZ) (1, 2). Trophoblast giant cells (TGCs), spongiotrophoblasts (spT), and syncytiotrophoblasts (SynTs) are the major cell types of fetal origin (1, 3). TGCs, which are the earliest differentiated cell type to form during embryogenesis in rodents, are essential for embryo implantation and maternal adaptations to pregnancy (1, 3). The SynT form two specialized cell layers (SynT-I and SynT-II) that encompass the entire surface of villous trees and the SynT-I cell layer is in direct contact with maternal blood in the maternal blood space (1, 3). The SynT layers prevent the exchange of large molecules and circulating cells between the fetus and the mother while enabling fetal nutrient uptake, waste elimination, and gas exchange through the maternal circulation (1, 3). Abnormalities in this maternal/fetal blood interface may result in various pregnancy-associated complications, such as recurrent miscarriage, preeclampsia (PE), and intrauterine growth restriction (IUGR) (1, 3). However, much remains unclear about the molecular mechanism by which the maternal and fetal blood interface is maintained during pregnancy.

Emerging evidence suggests that sphingolipids, a class of lipids containing a long-chain base (a sphingoid base) as a common moiety, have important roles in placental development and function. The biosynthesis of sphingolipids starts with the condensation of serine and palmitoyl-CoA through the action of serine palmitoyl-CoA transferase (SPT), which is followed by multiple sequential enzymatic steps . A recent study by Ding et al. (4) demonstrated that *SPTLC1, SPTLC2, and SPTSSA*, the genes encoding three SPT subunits, are markedly upregulated in mouse uterine stromal cells during decidualization and that inhibiting SPT with its inhibitor, I-cycloserine, results in defective decidualization and early pregnancy loss in mice. Sphingosine-1-phosphate (S1P), a sphingolipid metabolite, acts as a bioactive lipid that mediates various cellular responses (5), including cell proliferation (6–8), survival (8–10), differentiation (10), adhesion (11–13), and migration (14–17), mainly by activating one or more of its G protein-coupled receptors (GPCRs), $S1P_{1\text{-}5}$ (aka S1PR1-5) (18–22). S1P also mediates various biological processes including the maturation of the fetal vasculature (23), the development of heart (24), and angiogenesis (25) in mice. As such, deficiency of either S1P (26) or its receptor S1PR1 (23) leads to embryonic lethality. Recent studies find that S1P may mediate placental differentiation, development, and immunity. Mizugishi *et al.* (26) found that blocking the formation of endogenous S1P in mice impairs endometrial decidualization and severely compromises uterine blood vessels, leading to early pregnancy failure in mice. Mizugishi *et al.* also showed that inhibiting the formation of S1P induces massive infiltration of inflammatory cells into the fetoplacental unit (27).

Johnstone *et al.* (28) demonstrated that treatment with S1P inhibits the differentiation of primary human cytotrophoblasts into syncytiotrophoblasts *in vitro*. Yang *et al.* showed that S1P, when supplied exogenously, induces extravillous trophoblast cell invasion by activating S1PR1 (29). Westwood *et al.* demonstrated that S1P inhibits migration of human extravillous trophoblast cell lines (30). A recent study by Del Gaudio et al. (31) showed that S1P complexed with human cord blood-derived high-density-lipoprotein (HDL) preserves the integrity of the fetoplacental vasculature in an *in vitro* system. Similar to S1P, dihydrosphingosine-1-phosphate (DHS1P), a saturated analog of S1P, is abundant in blood (32) and can also activate S1PR1 in renal endothelial cells (33) although neither its role in placental development and function nor its regulation in the placenta are unclear. Although sphingolipids play important physiological roles in placental development and function, recent studies demonstrated that an aberrant elevation of placental sphingolipids may be implicated in pregnancy complications in humans, such as preeclampsia (PE) and intrauterine growth restriction (IUGR). Del Gaudio et al. (34) demonstrated that DHS, the immediate precursor of DHS1P, is increased in placental chorionic arteries and isolated endothelial cells from PE patients compared to healthy controls. Megan *et al.* (35) demonstrated that DHS is also increased in placentas from PE patients due to an increase in SPT activity. Chauvin *et al.* (36) found that the levels of sphingosine (SPH), the immediate precursor of S1P, are increased in IUGR placentas. Although the pathological role of SPH and DHS in placenta remains to be elucidated, both SPH and DHS, when accumulated in cells, have been shown to induce cell death (37, 38). Taken together, these results suggest that to ensure uneventful pregnancy, the metabolism of these bioactive sphingolipids in the placenta must be tightly regulated.

S1P and DHS1P are synthesized only from the phosphorylation of SPH and DHS, respectively, by the action of the SPH kinases, SPHK1 and SPHK2, in mammalian cells (39). SPH is in turn generated from the hydrolysis of ceramides by the action of ceramidases, which were classified into the acid, neutral, and alkaline ceramidase subtypes, respectively (40, 41). DHS is synthesized *de novo* from serine and palmitoyl-CoA by the sequential actions of serine palmitoyl transferase and ketodihydrosphingosine reductase or is generated from the hydrolysis of dihydroceramides by the action of ceramidase (40). We previously demonstrated that human alkaline ceramidase 2 (ACER2), a member of the alkaline ceramidase family that we identified initially from the yeast *Saccharomyces cerevisiae* and then from mammals, plays a key role in regulating S1P levels in cultured cells by catalyzing the generation of SPH, the rate-limiting step for S1P formation (42). Using genetically modified mouse models, we recently demonstrated that among the 5 known ceramidase genes, *ACER2* plays the predominant role in regulating the homeostasis of SPH, DHS, S1P, and DHS1P in plasma and several peripheral tissues (43). We previously demonstrated that the human *ACER2* is expressed at much higher levels in the placenta than in other major organs (44). However, it is unclear whether *ACER2* and its mouse counterpart *Acer2* play roles in regulating S1P and DHS1P levels in the placenta. Nor are clear its roles in placental development and function.

In this study, we demonstrate that the mouse *Acer2* is highly expressed in the placenta, similar to the human *ACER2*, and that *Acer2* plays a key role in regulating the placental levels of S1P and DHS1P by controlling the generation of SPH and DHS, respectively, in

both maternal and fetal cells in the placenta. Moreover, we reveal a novel role for the ACER2 pathway in maintaining the integrity of the maternal vasculature in the placenta and thereby fetal survival.

MATERIALS AND METHODS

Animals

The mouse strain (C57BL/6J-Acer2^{em1Mvw}/MvwJ JAX, stock 026793, abbreviated here to *Acer2*$^{+/-}$) heterozygous for an *Acer2* mutant allele in which exon 2 was deleted has been established in our previous study (43). The mouse strain (*Acer2*$^{-/-}$) homozygous for the *Acer2* mutant allele was generated by an intercross of *Acer2*$^{+/-}$ mice. Wild type C57BL/6 mice were purchased from The Jackson Laboratory. All mice used in this study were housed under conventional laboratory conditions of a constant room temperature (22°C), humidity level (55%), and 12-h light/dark photoperiod with mouse chow (W.F. Fisher & Son, Somerville, NJ) and water available *ad* libitum. For timed mating, male mice at ages of 2-5 months were housed individually for 1-2 weeks prior to mating with 2-5 month-old nulliparous female mice in proestrus or estrus. Female and male mice were paired at 6-7 pm and vaginal plugs were checked in the female mice next morning. If a copulatory plug was found, putative dams were separated from males. The morning that a plug was found was set as 0.5 *days post coitum* (0.5 dpc) or embryonic day 0.5 (E0.5). The plugged mice were weighed daily to confirm successful pregnancy. Female mice lacking copulatory plugs were re-paired with male mice until a copulatory plug was spotted. Mice were weaned at 21 days of age and genotyped by PCR as described (43). All animal studies were performed following procedures approved by the Institutional Animal Care and Use Committee (IACUC) at Stony Brook University (Stony Brook, NY) and comply with National Institutes of Health (NIH) guidelines.

Quantitative PCR (qPCR)

RNAs were extracted from tissues using a Trizol™ plus RNA purification kit with the catalog number (Cat. #) 12183555 from Thermo Fisher Scientific Inc. (Thermo-Fisher), Waltham, MA, USA, and reversely transcribed into cDNAs using Superscript™ III First-Strand Synthesis SuperMix (Cat. # 18080400, Thermo-Fisher) as described in our previous study (43). cDNAs were subjected to qPCR that was performed on an ABI Prism 7000 system (Thermo-Fisher). mRNA levels were analyzed using Q-Gene software which expresses data as mean normalized expression (MNE) (45). MNE is directly proportional to the mRNA levels of a target gene relative to those of the reference gene (β-actin). The primers for qPCR were synthesized by Integrated DNA Technologies, Inc. (Coralville, IA, USA) and listed in Table 1.

Histology

Fetoplacental units were harvested at different dpc, fixed in 10% formalin (Thermo-Fisher, Waltham, MA), dehydrated in a graded series of ethanol (Thermo-Fisher) and xylene (Thermo-Fisher), followed by infiltration of melted paraffin (Thermo-Fisher) at 56°C in an automated processor. The tissues embedded in paraffin were sectioned vertically (the chorionic plate providing the theoretical horizontal plane) at a thickness of 7 μm as

described (46), and tissue sections were mounted on SuperFrost® Plus slides (Thermo-Fisher Scientific). The tissue sections were baked, deparaffined, and rehydrated before being stained with a hematoxylin and eosin (H&E) solution (Sigma-Aldrich, St. Louis, MO) or with a Periodic acid–Schiff stain (PAS) solution (Cat. # 150680, Abeam, Cambridge, MA) as per the manusfecturer's instructions. The stained tissue sections that were close to the placental midline and exhibited the largest area among the serial sections were imaged under an Olympus BX53 fluorescent microscope (Olympus Corporation of the Americas, Center Valley, PA).

In situ hybridization

Fetoplacental unit sections were prepared as described above and subjected to in situ hybridization with an RNAscope probe specific for the mouse gene *Acer2* (Cat. # 493281) or *Tpbpa* (Cat. # 405511), which both were designed and manufactured by Advanced Cell Diagnostics (ACD (Newark, CA, USA). Briefly, tissue sections were baked and deparaffinized on the instrument, followed by epitope retrieval (using Leica Epitope Retrieval Buffer 2 at 95°C or at 88°C for 15 min) and protease treatment (15 min at 40°C). Probe hybridization, signal amplification, colorimetric detection, and counterstaining were subsequently performed using RNAscope® 2.5 HD reagent kits (ACD) as per the manufacturer's instructions. The stained tissue sections were imaged under the Olympus BX53 fluorescent microscope. Brown or red dots in cells represent mRNA molecules of the genes Acer2 and Tpbpa, respectively.

Immunohistochemistry (IHC)

IHC was performed with paraffin-embedded sections as described in our previous study (47). Briefly, tissue sections were deparaffined, rehydrated, retrieved antigens, and quenched endogenous peroxidase activity. Sections were stained with 2 μg/ml of biotinylated *Griffonia simplicifolia* lectin I isolectin B4 (IB4) (Cat.# B-1205, Vector Laboratories, Burlingame, CA) in PBS, followed by HRP-conjugated streptavidin (1:4000) (Thermo-Fisher). Finally, the tissue sections were incubated with 1.1 mM 3,3'-Diaminobenzidine tetrahydrochloride hydrate (DAB) (Cat. # D5637, Sigma-Aldrich), and counterstained with hematoxylin (Cat. # HHS32, Sigma-Aldrich). The stained tissue sections were imaged under the Olympus BX53 fluorescent microscope.

Quantitative analyses of stained tissue sections

The software Fiji, an open source image processing package based on ImageJ (Media Cybernetics, Inc., Rockville, MD, USA), was used to measure the staining intensities or the area fractions of H&E, IHC, or ISH-stained tissue sections. Briefly, the microscopic image of each tissue section stained with H&E, IHC, or ISH was converted into an 8-bit grayscale image, the threshold of which was adjusted to match the stained areas in the original image. In the threshholded images, the total placental section area was marked using the 'free-hand selections' tool, and the area fraction, i.e., the percentage of the specifically stained area to the total tissue section area, was obtained using the 'measure' tool under the 'Analyze' panel in Fiji. To quantify ISH signals in cells in sections stained for *Acer2* mRNA, raw integrated densities (IntDen) in individual cells were obtained in the thresholded images. The *Acer2* mRNA levels in each cell were expressed as an average pixel intensity (pixels per cell).

Western blot analysis

Total cell membranes were isolated from mouse placental tissues as described in our previous study (47). Proteins were extracted from the cell membranes, measured using a Pierce™ BCA Protein Assay Kit (Cat.# 23225, Thermo-Fisher) and resolved on 12% polyacrylamide gels before being transferred to nitrocellulose (NC) membranes. The NC membranes were probed with the house-made anti-ACER2 antibody followed by the secondary antibody, goat anti-rabbit IgG antibody conjugated with horseradish peroxidase (HRP) (Cat.# 7074s, Cell Signaling Technology, Danvers, MA, USA). The ACER2 protein bands were detected with an Enhanced Chemiluminescence (ECL) kit (Cat.# PI32106, Thermo-Fisher). The ACER2 antibody was stripped off the NC membranes, which were re-probed with anti-GM130 antibody (Cat. # NBP2-53420, Novus Biologicals, Littleton, CO, USA) at a 1:1000 dilution, followed by the secondary antibody-HRP conjugate before the GM130 protein band was detected with the ECL kit. The ACER2 and GM130 protein bands were scanned and the density ratios of ACER2 protein bands to GM130 bands were measured using the software ImageJ. Briefly, the background was first subtracted from the scanned image using ImageJ's built-in "subtract background" feature. Then the rectangle tool was used to select the ACER2 row as the first lane and then plot the lane. On the graph plot of the row, the lowest points of each peak were connected and the peak area was recorded using the wand tool. The same steps were repeated for the GM130 row to obtain the peak area of each GM130 band. Finally, the data from ImageJ were copied and pasted into an Excel spreadsheet, and the density ratio of the ACER2 protein band to the GM130 band from each sample was computed.

Sphingolipid analysis

Placental tissues collected from mice at different gestation days were subjected to LC-MS/MS analyses for various sphingolipids as described in our previous study (43). Levels of sphingolipids were normalized to total protein in each sample.

Statistical analysis

Data were presented as the mean ± SD and statistically analyzed by two-tailed and unpaired *t*-test or one-way ANOVA using the software GraphPad Prism 8 (GraphPad Software Inc., San Diego, CA, USA). A difference with a $p\ value < 0.05$ is considered significant.

RESULTS

The mouse alkaline ceramidase 2 gene (Acer2) is highly expressed in multiple cell types in the placenta during placental development

With Northern blot analysis, we previously demonstrated that the human gene *ACER2* is highly expressed in the placenta (44). To determine whether this is also the case with the mouse alkaline ceramidase 2 gene, *Acer2*, we compared *Acer2* mRNA levels in the placenta to those in other major organs in mice. We isolated total RNA from placentas at embryonic day 12.5 (E12.5), a time when all the three cellular layers of the placenta have been well established, and other major organs from the mothers, including brain, heart, lung, liver, kidney, spleen, colon, stomach, and thymus from pregnant C57BL/6J females. The RNA

samples were subjected to qPCR analysis with a primer pair specific for *Acer2* or β-actin gene. The qPCR results showed that *Acer2* mRNA levels are the highest in the placenta among the tissues that we examined (Fig. 1A), suggesting that similar to its human counterpart (*ACER2*), the mouse gene *Acer2* is also highly expressed in the placenta.

For a better understanding of the role of *Acer2* in placental development and function, we investigated spatiotemporal expression of *Acer2* in the placenta. We first determined its temporal expression. Total RNA and protein were extracted from placentas at different embryonic days before *Acer2* mRNA and protein levels were determined by qPCR and Western blot analysis, respectively. We found that placental *Acer2* mRNA levels were high at E9.5 to E12.5 but nearly undetectable at E13.5 and E15.5 (Figure 1B). Consistently, ACER2 protein was readily detected in placentas at E9.5 to E12.5 but it was expressed only slightly in E13.5 placentas (Figure 1C and 1D). These results suggest that *Acer2* is highly expressed in the placenta during its development. We then determined its spatial expression in the placentas by *in-situ* hybridization (ISH). Fetoplacental units at E11.5, a time when placental *Acer2* mRNA levels peak, were dissected from $Acer2^{+/+}$ pregnant dams crossed with $Acer2^{+/+}$ males, fixed, paraffin-embedded, and sectioned. Sections from one of the fetoplacental units were processed for ISH, which was performed with the *Acer2*-specific ACD RNAscope probe. The results showed that *Acer2* was highly expressed in decidual stromal cells (DC) (Figure 2A, 2B, and 2C), spongiotrophoblasts (JZT) (Figure 2A, 2B, and 2D), various trophoblast giant cells (TGCs) (Figure 2A, 2B, and 2E), labyrinthine trophoblasts (LZT) (Figure 2A, 2B, and 2F), and but not fetal endothelial cells (EC) (Figure 2A, 2B, and 2G), suggesting that Acer2 is highly expressed in most major placental cell lineages in the placenta.

Deficiency of Acer2 in both the mother and fetus reduces litter size

As the mouse placenta resembles the human placenta in both architecture and function (2), analyses of mutant mice deficient in the mouse *Acer2* gene would enable a better understanding of the roles for this enzyme in placental development and function in mammals. We previously generated a mouse strain ($Acer2^{+/-}$) heterozygous for the *Acer2* mutant allele lacking exon 2 using the CRISPR/Cas9 genomic editing technology (43). We also demonstrated that intercrosses of $Acer2^{+/-}$ mice produced a similar number of live-born neonates per litter to intercrosses of wild-type ($Acer2^{+/+}$) mice and that a similar number of offspring *per litter* (litter size) was weaned from intercrosses of $Acer2^{+/-}$ or $Acer2^{+/+}$ (43). These results suggest that female heterozygotes are fertile and that total *Acer2* deficiency in the placental cell lineages of fetal origin affects neither placental development and function nor fetal development and survival.

As the placenta consists of the cell lineages of both maternal and fetal origins (3), we next tested whether *Acer2* deficiency in the mother impairs fetal development and survival by crossing $Acer2^{-/-}$ females with $Acer2^{+/+}$ males. The crosses of $Acer2^{-/-}$ females and $Acer2^{+/+}$ males delivered a similar number of live-born neonates per litter to the intercrosses of $Acer2^{+/+}$ females and males (Figure 3), suggesting that ablating the *Acer2* gene only from the maternal components of the placenta does not affect placental development and function either.

We then determined whether *Acer2* deficiency in both mother and fetus impairs fetal development and survival by intercrosses of $Acer2^{-/-}$ mice. We observed that the intercrosses of $Acer2^{-/-}$ mice delivered 50% fewer live-born neonates per litter than the intercrosses of $Acer2^{+/+}$ mice did (Figure 3), suggesting that *Acer2* deficiency in both mother and fetus impairs fetal development and/or survival at 50% penetrance.

Acer2 deficiency in both mother and fetus results in placental hemorrhages and partial embryonic lethality

To investigate at what stage *Acer2* deficiency impaired fetal development and/or survival, we performed necropsy of $Acer2^{-/-}$ and $Acer2^{+/+}$ pregnant dams that were intercrossed with $Acer2^{-/-}$ and $Acer2^{+/+}$ males, respectively, at different stages of pregnancy. By inspecting whole uteri, we found no differences in the number, size, gross morphology, and spacing of E10.5 or E11.5 fetoplacental units in the uteri of pregnant $Acer2^{-/-}$ and $Acer2^{+/+}$ dams (Figure 4A). However, 50% of E12.5 fetoplacental units were dark-colored and being absorbed in the uteri of $Acer2^{-/-}$ pregnant dams compared to those in the uteri of $Acer2^{+/+}$ pregnant dams (Figure 4A). By dissecting uteri and inspecting individual fetoplacental units, we found that all E11.5 $Acer2^{-/-}$ E11.5 $Acer2^{+/+}$, and E12.5 $Acer2^{+/+}$ fetuses had a heartbeat and thereby survived whereas ≈50% of E12.5 $Acer2^{-/-}$ fetuses died and/or absorbed (Figure 4B and 4C).

Macroscopic examination revealed numerous blood pools within 50% of E12.5 $Acer2^{-/-}$ placentas but not in any E12.5 $Acer2^{+/+}$ placenta (Figure 5A), indicating that *Acer2* deficiency causes hemorrhages in the placenta at E12.5. To define where hemorrhages occurred exactly in the placenta, we histologically analyzed hemorrhagic E12.5 placentas from $Acer2^{-/-}$ pregnant dams bred to $Acer2^{-/-}$ males and E12.5 placentas from $Acer2^{+/+}$ pregnant dams bred to $Acer2^{+/+}$. We observed the presence of massive hemorrhages of maternal blood in the Jz and Lz in the $Acer2^{-/-}$ placentas but not in $Acer2^{+/+}$ placentas (Figure 5B, 5C, and 5D). Quantitative analysis with Image J showed that the bleeding area was markedly increased in the $Acer2^{-/-}$ placenta compared to the $Acer2^{+/+}$ placenta (Figure 5E). These results suggest that *Acer2* deficiency in both the mother and fetus results in partial embryonic lethality likely due to placental hemorrhages.

Hemorrhages due to Acer2 deficiency result in expansion of P-TGC and atrophy of both junctional zone and fetal vascular network in the labyrinthine zone

The placenta contains various types of differentiated trophoblast cells, including trophoblast giant cells (TGC), spongiotrophoblasts, glycogen trophoblasts, and labyrinthine trophoblasts; each subclass trophoblasts has its unique gene expression signatures (3). To investigate whether *Acer2* deficiency affects the differentiation of these trophoblast cell types, we investigated whether *Acer2* deficiency affected the formation of the three distinct cellular layers of the placenta. Periodic acid-Schiff (PAS) staining showed that the population of P-TGCs was increased in the hemorrhagic E12.5 $Acer2^{-/-}$ placentas (Figure 6A, 6B, and 6E). The expansion of P-TGCs was confirmed with *in situ* hybridization (ISH) with an RNA probe specific for *Prl2c2*, a marker gene of P-TGCs (Figure 6C, 6D, and 6F). ISH with a *Tpbpa*-specific RNA probe showed that the area of the Jz was markedly reduced in the $Acer2^{-/-}$ placentas compared to the $Acer2^{+/+}$ placentas and non-hemorrhagic $Acer2^{-/-}$

placentas (Figure 6G, 6H, and 6K). Labeling with biotinylated isolectin B4 (IB4), which specifically binds the endothelial cell surface of the blood vessels of fetal origin, revealed that the capillary network was strongly diminished in in the hemorrhagic *Acer2*$^{-/-}$ placenta compared to either *Acer2*$^{+/+}$ or non-hemorrhagic Acer2$^{-/-}$ placenta (Figure 6I, 6J, and 6L). These results suggest that *Acer2* deficiency causes the maternal blood hemorrhage, which in turn alters the placental architecture.

Acer2 deficiency does not affect the expression of genes that mark the major placental cell types during placental development

To investigate whether *Acer2* deficiency impaired the differentiation of the placental cell lineages, we performed qPCR analyses of genes that mark major cell types in the placenta at E11.5, which is the time when all the three distinct cellular layers of the placenta have been established. We found no difference in the mRNA levels of placental cell marker genes between *Acer2*$^{+/+}$ and *Acer2*$^{-/-}$ placentas, including the genes specific for decidual stromal cells (*Prl8a2*) (Figure 7A) and spiral artery TGCs (*Prl7b1*) (Figure 7B) in the Dz, parietal TGCs (*Prl3d1*) in the fetomaternal interface (Figure 7C), spongiotrophoblasts (*Tpbpa*) (Figure 7D), glycogen trophoblasts (*Tpbpa*) (Figure 7D), channel TGCs (*Ctsq*) (Figure 7E), and canal TGCs (*Prl3b1*) in the Jz (Figure 7F), sinusoidal TGCs (*Ctsq*) (Figure 7E), syncytiotrophoblast I (*SynA*) (Figure 7G), syncytiotrophoblast II (*SynB*) (Figure 7H), and fetal endothelial cells (*Pecam1*) in the Lz (Figure 7I), suggesting that Acer2 deficiency does not affect the differentiation of the placental cell lineages.

Acer2 deficiency in both the mother and fetus reduces the placental levels of sphingolipids

To investigate whether Acer2 KO disrupts the integrity of the placental vasculature by breaching the homeostasis of sphingolipids in this extraembryonic organ, we measured the levels of sphingolipids, including ceramides, dihydroceramides, sphingoid bases, and sphingoid base phosphates in *Acer2*$^{+/+}$ or *Acer2*$^{-/-}$ placentas. LC-MS/MS analyses demonstrated that knocking out *Acer2* from both the mother and fetus significantly decreased the levels of SPH (Figure 8A), DHS (Figure 8B), S1P (Figure 8C), DHS1P (Figure 8D), and dihydroceramides (Figure 8E) without affecting the levels of ceramides (Figure 8F) in either hemorrhagic or non-hemorrhagic placentas at E12.5. Interestingly, the levels of both SPH and S1P were higher in the non-hemorrhagic placenta than in the hemorrhagic placenta. To investigate whether the differences in the levels of SPH and S1P resulted from a compensatory effect of another alkaline ceramidase 3 (ACER3) that is expressed in the placenta, we measured *Acer3* mRNA levels in *Acer2*$^{+/+}$ placentas, hemorrhagic and non-hemorrhagic *Acer2*$^{-/-}$ placentas. With qPCR analysis, we showed that the *Acer3* mRNA levels were elevated in the non-hemorrhagic *Acer2*$^{-/-}$ placentas compared to either the Acer2$^{+/+}$ placenta or the hemorrhagic *Acer2*$^{-/-}$ placenta (Figure 8G). These results suggest that *Acer2* deficiency in both the mother and fetus alters the homeostasis of sphingoid bases (SPH and DHS) and their phosphates (S1P and DHS1P) in the placenta and that a compensatory upregulation of another alkaline ceramidase in the same protein family enables some but not all *Acer2*$^{-/-}$ placentas to develop and function normally.

DISCUSSION

The placenta in rodents and humans has both maternal and fetal vascular systems that come in close proximity to enable nutrient and gas exchange between the mother and fetus (3). Successful establishment and maintenance of both vasculature systems in the placenta are critical for fetal development and survival (48). S1P has been long known for its role in maintaining the integrity of the embryonic vasculature in mice (49) but neither its regulation in the placenta nor its role in regulating the placental vasculature were clear. In this study, we report two principle findings: 1) we identified the mouse ACER2 as a key regulator of the placental levels of S1P, DHS1P (the saturated analog of S1P), and their precursors (SPH and DHS); and 2) we demonstrated that ACER2 plays an important role in maintaining the integrity of the maternal vasculature in the mouse placenta .

Our previous and current data suggest that ACER2 is highly expressed in both human and mouse placentas. Via both Northern blot and qPCR analyses, we previously demonstrated that human *ACER2* mRNA levels are the highest in the placenta among major organs that we examined (44). This is also true with mouse *Acer2* mRNA levels, as demonstrated in this study. The placenta with the three cellular layers, the Dz, Jz, and Lz, is formed at E9.5 and fully mature by E14.5 (3). Both qPCR and Western blot analyses revealed that *Acer2* is expressed in the placenta between E9.5 and E12.5 (Figure 1), suggesting that Acer2 is expressed in the placenta at its early developmental stage. Histology revealed that *Acer2* deficiency does not affect the formation of the three distinct cellular layers in the placenta at E12.5 (Figure 5). Consistently, qPCR analyses revealed no difference in the mRNA levels of genes that mark the major cell lineages in the placenta at E11.5 (Figure 6), a time when all the three cellular layers have been well established but not fully mature. These results suggest that *Acer2* expression in the placenta is not required for the early specification of the placental cell lineages. However, *Acer2* deficiency in both the mother and fetus caused hemorrhages from the maternal but not fetal vasculature in an approximately 50% of E12.5 placentas (Figure 4), suggesting that *Acer2* is required for the integrity of the maternal but not fetal vasculature in the placenta. *Acer2* deficiency in either the mother or fetus does not impair fetal survival (Figure 3), indicating that *Acer2* expression either in the mother or fetus is sufficient for maintaining the integrity of the maternal vasculature.

The placental dysfunction phenotype is not fully penetrant on this background. *We analyzed the sex ratio of live pups from the intercrossing of Acer2*$^{-/-}$ *mice (6 pairs) and found that the ratio is 1:1 (data not shown). This suggests that the phenotype of hemorrhage is independent of fetal or placental sex*. Our results indicate that ACER3, another member in the same protein family as ACER2, may compensate for loss of *Acer2* in the placenta in mice that survive beyond E13.5. As a future direction, we will test whether loss of both *Acer2* and *Acer3* would increase penetrance in the placental defective phenotype in mice.

In primates and rodents, the fetal vasculature is lined with endothelial cells whereas the maternal vascular space in the placenta is unique in that, unlike other organs, placenta-derived trophoblast giant cells (TGCs) but not endothelial cells line the maternal side of the vasculature (1). There are several types of TGCs, including spiral artery TGCs (SpA-TGCs), canal TGCs (C-TGCs), channel TGCs (Ch-TGCs), and sinusoidal TGCs (S-TGCs) (1). ISH

revealed high expression of *Acer2* in fetal TGCs but not in fetal endothelial cells in the placenta (Figure 2). This cell type-specific expression is in line with its role in maintaining the integrity of the maternal vasculature but not the fetal vasculature in the placenta.

Interestingly, *Acer2* deficiency leads to the expansion of P-TGCs with a concomitant atrophy of Jz and the fetal capillary network in Lz in hemorrhagic placentas but not in non-hemorrhagic placenta at E12.5 (Figure 5). These results suggest that the unregulated expansion of the P-TGC layer and the atrophy of both Jz and Lz may be the consequences rather than the causes of hemorrhages of the maternal blood in *Acer2*-deficient placentas. However, the atrophy of the Jz and Lz may limit the influx of nutrients from the mother to the fetus and the waste discharge from the fetus to the mother through circulation, thus leading to embryonic lethality.

As we previously demonstrated that ACER2 plays a critical role in the homeostasis of sphingoid bases (SPH and DHS) and sphingoid base phosphates (S1P and DHS1P) in several tissues in adult mice (43), its predominant expression in the placenta is expected to be pivotal for the homeostasis of these bioactive lipids in the this temporary organ. Indeed, in this current study, we demonstrated that generating nulls for both *Acer2 alleles* in both the mother and embryo markedly decreased the levels of SPH, DHS, S1P, and DHS1P in the placenta (Figure 7). In addition to the role of ACER2 in regulating S1P and DHS1P in peripheral tissues, we previously demonstrated that ACER2 plays a key role in regulating circulating SBPs (43). These results suggest that SBPs in the fetal components of the placenta are generated locally from major placental cell types and supplied systemically from the circulation. Plasma S1P has been shown to play a key role in the maturation of the fetal vasculature in mice by mediating the interaction between endothelial cells and mural cells (23) and the formation of adherens junctions between endothelial cells (50, 51). S1P mediates these biological processes mainly by activating S1PR1, one of the 5 S1P-specific G protein-coupled receptors (51). In contrast to S1P, the role of DHS1P in the vascular system is largely unclear. As DHS1P has been shown to activate S1PR1 in renal endothelial cells (33), we predict that DHS1P may have the same role as S1P in maintaining the integrity of the vasculature lined with endothelial cells. S1P and DHS1P may regulate the integrity of the maternal vasculature lined with TGCs in the placenta by activating S1PR1 in these cells. If this is the case, *Acer2* deficiency may disrupt trophoblast and trophoblast adhesion by inhibiting the S1P/DHS1P-S1PR1 pathway, thus resulting in the leakage of the maternal blood space.

Most of pregnancy complications in humans, such as PE and IUGR, are associated with defects in the placental vasculature. As mentioned earlier, placental levels of SPH or DHS are elevated in patients with either IUGR (36) or PE (35). As both SPH and DHS are highly cytotoxic, their accumulation may lead to cell death in the placenta. In line with this notion, generating nulls for both *Sphk1* alleles and a single *Sphk2* allele impaired decidualization due to an aberrant accumulation of SPH and DHS, thus resulting in embryonic lethality (26). These results suggest that as the immediate precursors of sphingoid base phosphates, SPH and DHS are essential for the vasculature integrity whereas their aberrant increases may induce apoptosis of cells in the placenta, thus breaching placental integrity and/or placental atrophy.

These results suggest that the human ACER2, as a key regulator of both SPH and DHS, must be tightly regulated in the placenta during uneventful pregnancy. Therefore, it would be interesting to know whether an aberrant activation or upregulation of ACER2 contributes to the breaching of the homeostasis of these bioactive sphingolipids in the placentas in patients with PE, IUGR, or other pregnancy complications.

Although we have made great strides in understanding the role of ACER2 in regulating the hemostasis of bioactive sphingolipids in the placenta and the integrity of the placental vasculature, there are several limitations of this study. One limitation is that our current mouse model does not allow us to define the placental cell lineage-specific role of ACER2 in regulating the integrity of the placental vasculature as *Acer2* is inactivated globally in $Acer2^{-/-}$ mice. Another limitation is that it is impossible to define the relative contribution of each of the bioactive lipids that are regulated by ACER2 to the integrity of the placental vasculature as several bioactive lipids, including S1P, DHS1P, and their precursors were perturbed in $Acer2^{-/-}$ knockout mice. Another limitation is that we do not know whether the adaptive upregulation of Acer3 is indeed accountable for the incomplete penetrance of the placental phenotype of $Acer2^{-/-}$ mice. As a future direction, these limitations will be addressed using more sophisticated animal models that we are planning to generate.

In conclusion, ACER2 is a key regulator of the homeostasis of placental bioactive sphingolipids, and its expression is important for the integrity of the maternal blood space in the placenta (Figure 9). This study may lead to novel approaches to prevention and/or treatment of many pregnancy complications, such as PE and IUGR.

Supplementary Material

Refer to Web version on PubMed Central for supplementary material.

ACKNOWLEDGEMENTS

We thank Dr. Izolda Mileva and Dr. Ashley Snider for assistance with sphingolipid analyses and animal maintenance, respectively. This work was supported, in whole or in part, by National Institutes of Health Grants R01CA163825 (to C.M) and P01CA097132 (to Y.A.H and C.M), the National Natural Science Foundation of China grant 81770529 (to Y.C), and The Guangdong Gastrointestinal Disease Research Center grant 2017B020209003 (to Y.C). This work was also supported by the Sphingolipid Animal Cancer Pathobiology Shared Resource Core and the Lipidomics Shared Resource Core at Stony Brook University.

ABBREVIATIONS:

ACER2	alkaline ceramidase 2
ACER3	alkaline ceramidase 3
ASAH1	acid ceramidase
Cer	ceramide
dhCer	dihydroceramide
dhSPH	dihydrosphingosine

dhS1P	dihydrosphingosine-1-phophate
dpc	days post coitum
Dz	decidual zone
GPRC	G protein-coupled receptor
ISH	in-situ hybridization
IUGR	intrauterine growth restriction
Jz	junctional zone
Lz	labyrinthine zone
PE	preeclampsia
SBP	sphingoid base-1-phosphate
SPH	sphingosine
S1PR1	S1P receptor 1
S1P	sphingosine-1-phosphate
spT	spongiotrophoblasts
SynT	syncytiotrophoblasts
TGC	trophoblast giant cell

REFERENCES

1. Woods L, Perez-Garcia V, and Hemberger M (2018) Regulation of Placental Development and Its Impact on Fetal Growth-New Insights From Mouse Models. Frontiers in endocrinology 9, 570 [PubMed: 30319550]
2. Malassine A, Frendo JL, and Evain-Brion D (2003) A comparison of placental development and endocrine functions between the human and mouse model. Human reproduction update 9, 531–539 [PubMed: 14714590]
3. Hemberger M, Hanna CW, and Dean W (2020) Mechanisms of early placental development in mouse and humans. Nature reviews. Genetics 21, 27–43
4. Ding NZ, Qi QR, Gu XW, Zuo RJ, Liu J, and Yang ZM (2018) De novo synthesis of sphingolipids is essential for decidualization in mice. Theriogenology 106, 227–236 [PubMed: 29096270]
5. Spiegel S, and Milstien S (2003) Sphingosine-1-phosphate: an enigmatic signalling lipid. Nat Rev Mol Cell Biol 4, 397–407 [PubMed: 12728273]
6. Zhang H, Desai NN, Olivera A, Seki T, Brooker G, and Spiegel S (1991) Sphingosine-1-phosphate, a novel lipid, involved in cellular proliferation. J Cell Biol 114, 155–167. [PubMed: 2050740]
7. Kluk MJ, and Hla T (2001) Role of the sphingosine 1-phosphate receptor edg-1 in vascular smooth muscle cell proliferation and migration. Circ Res 89, 496–502. [PubMed: 11557736]
8. Van Brocklyn JR, Lee MJ, Menzeleev R, Olivera A, Edsall L, Cuvillier O, Thomas DM, Coopman PJ, Thangada S, Liu CH, Hla T, and Spiegel S (1998) Dual actions of sphingosine-1-phosphate: extracellular through the Gi-coupled receptor Edg-1 and intracellular to regulate proliferation and survival. J Cell Biol 142, 229–240. [PubMed: 9660876]

9. Cuvillier O, Pirianov G, Kleuser B, Vanek PG, Coso OA, Gutkind S, and Spiegel S (1996) Suppression of ceramide-mediated programmed cell death by sphingosine-1-phosphate. Nature 381, 800–803. [PubMed: 8657285]
10. Edsall LC, Pirianov GG, and Spiegel S (1997) Involvement of sphingosine 1-phosphate in nerve growth factor-mediated neuronal survival and differentiation. The Journal of neuroscience: the official journal of the Society for Neuroscience 17, 6952–6960. [PubMed: 9278531]
11. Wiltshire R, Nelson V, Kho DT, Angel CE, O'Carroll SJ, and Graham ES (2016) Regulation of human cerebro-microvascular endothelial baso-lateral adhesion and barrier function by S1P through dual involvement of S1P1 and S1P2 receptors. Scientific reports 6, 19814 [PubMed: 26813587]
12. Ko P, Kim D, You E, Jung J, Oh S, Kim J, Lee KH, and Rhee S (2016) Extracellular Matrix Rigidity-dependent Sphingosine-1-phosphate Secretion Regulates Metastatic Cancer Cell Invasion and Adhesion. Scientific reports 6, 21564 [PubMed: 26877098]
13. Lin CC, Lee IT, Hsu CH, Hsu CK, Chi PL, Hsiao LD, and Yang CM (2015) Sphingosine-1-phosphate mediates ICAM-1-dependent monocyte adhesion through p38 MAPK and p42/p44 MAPK-dependent Akt activation. PLoS One 10, e0118473 [PubMed: 25734900]
14. Wang F, Van Brocklyn JR, Hobson JP, Movafagh S, Zukowska-Grojec Z, Milstien S, and Spiegel S (1999) Sphingosine 1-phosphate stimulates cell migration through a G(i)-coupled cell surface receptor. Potential involvement in angiogenesis. J Biol Chem 274, 35343–35350. [PubMed: 10585401]
15. Hobson JP, Rosenfeldt HM, Barak LS, Olivera A, Poulton S, Caron MG, Milstien S, and Spiegel S (2001) Role of the sphingosine-1-phosphate receptor EDG-1 in PDGF-induced cell motility. Science 291, 1800–1803. [PubMed: 11230698]
16. Paik JH, Chae S, Lee MJ, Thangada S, and Hla T (2001) Sphingosine 1-phosphate-induced endothelial cell migration requires the expression of EDG-1 and EDG-3 receptors and Rho-dependent activation of alpha vbeta3- and beta1-containing integrins. J Biol Chem 276, 11830–11837. [PubMed: 11150298]
17. Van Brocklyn JR, Young N, and Roof R (2003) Sphingosine-1-phosphate stimulates motility and invasiveness of human glioblastoma multiforme cells. Cancer Lett 199, 53–60 [PubMed: 12963123]
18. Lee MJ, Van Brocklyn JR, Thangada S, Liu CH, Hand AR, Menzeleev R, Spiegel S, and Hla T (1998) Sphingosine-1-phosphate as a ligand for the G protein-coupled receptor EDG-1. Science 279, 1552–1555. [PubMed: 9488656]
19. Sanchez T, and Hla T (2004) Structural and functional characteristics of S1P receptors. J Cell Biochem 92, 913–922 [PubMed: 15258915]
20. Proia RL, and Hla T (2015) Emerging biology of sphingosine-1-phosphate: its role in pathogenesis and therapy. J Clin Invest 125, 1379–1387 [PubMed: 25831442]
21. Mendelson K, Evans T, and Hla T (2014) Sphingosine 1-phosphate signalling. Development 141, 5–9 [PubMed: 24346695]
22. Blaho VA, and Hla T (2014) An update on the biology of sphingosine 1-phosphate receptors. J Lipid Res 55, 1596–1608 [PubMed: 24459205]
23. Liu Y, Wada R, Yamashita T, Mi Y, Deng CX, Hobson JP, Rosenfeldt HM, Nava VE, Chae SS, Lee MJ, Liu CH, Hla T, Spiegel S, and Proia RL (2000) Edg-1, the G protein-coupled receptor for sphingosine-1-phosphate, is essential for vascular maturation. J Clin Invest 106, 951–961. [PubMed: 11032855]
24. Clay H, Wilsbacher LD, Wilson SJ, Duong DN, McDonald M, Lam I, Park KE, Chun J, and Coughlin SR (2016) Sphingosine 1-phosphate receptor-1 in cardiomyocytes is required for normal cardiac development. Developmental biology 418, 157–165 [PubMed: 27333774]
25. Lee MJ, Thangada S, Claffey KP, Ancellin N, Liu CH, Kluk M, Volpi M, Sha'afi RI, and Hla T (1999) Vascular endothelial cell adherens junction assembly and morphogenesis induced by sphingosine-1-phosphate. Cell 99, 301–312. [PubMed: 10555146]
26. Mizugishi K, Li C, Olivera A, Bielawski J, Bielawska A, Deng CX, and Proia RL (2007) Maternal disturbance in activated sphingolipid metabolism causes pregnancy loss in mice. J Clin Invest 117, 2993–3006 [PubMed: 17885683]

27. Mizugishi K, Inoue T, Hatayama H, Bielawski J, Pierce JS, Sato Y, Takaori-Kondo A, Konishi I, and Yamashita K (2015) Sphingolipid pathway regulates innate immune responses at the fetomaternal interface during pregnancy. J Biol Chem 290, 2053–2068 [PubMed: 25505239]
28. Johnstone ED, Chan G, Sibley CP, Davidge ST, Lowen B, and Guilbert LJ (2005) Sphingosine-1-phosphate inhibition of placental trophoblast differentiation through a G(i)-coupled receptor response. J Lipid Res 46, 1833–1839 [PubMed: 15995175]
29. Yang W, Li Q, and Pan Z (2014) Sphingosine-1-phosphate promotes extravillous trophoblast cell invasion by activating MEK/ERK/MMP-2 signaling pathways via S1P/S1PR1 axis activation. PLoS One 9, e106725 [PubMed: 25188412]
30. Westwood M, Al-Saghir K, Finn-Sell S, Tan C, Cowley E, Berneau S, Adlam D, and Johnstone ED (2017) Vitamin D attenuates sphingosine-1-phosphate (S1P)-mediated inhibition of extravillous trophoblast migration. Placenta 60, 1–8 [PubMed: 29208234]
31. Del Gaudio I, Sreckovic I, Zardoya-Laguardia P, Bernhart E, Christoffersen C, Frank S, Marsche G, Illanes SE, and Wadsack C (2020) Circulating cord blood HDL-S1P complex preserves the integrity of the feto-placental vasculature. Biochimica et biophysica acta. Molecular and cell biology of lipids 1865, 158632 [PubMed: 31954174]
32. Li F, Xu R, Low BE, Lin CL, Garcia-Barros M, Schrandt J, Mileva I, Snider A, Luo CK, Jiang XC, Li MS, Hannun YA, Obeid LM, Wiles MV, and Mao C (2018) Alkaline ceramidase 2 is essential for the homeostasis of plasma sphingoid bases and their phosphates. Faseb j 32, 3058–3069 [PubMed: 29401619]
33. Park SW, Kim M, Chen SW, Brown KM, D'Agati VD, and Lee HT (2010) Sphinganine-1-phosphate protects kidney and liver after hepatic ischemia and reperfusion in mice through S1P1 receptor activation. Laboratory investigation; a journal of technical methods and pathology 90, 1209–1224 [PubMed: 20458275]
34. Del Gaudio I, Sasset L, Lorenzo AD, and Wadsack C (2020) Sphingolipid Signature of Human Feto-Placental Vasculature in Preeclampsia. International journal of molecular sciences 21
35. Melland-Smith M, Ermini L, Chauvin S, Craig-Barnes H, Tagliaferro A, Todros T, Post M, and Caniggia I (2015) Disruption of sphingolipid metabolism augments ceramide-induced autophagy in preeclampsia. Autophagy 11, 653–669 [PubMed: 25853898]
36. Chauvin S, Yinon Y, Xu J, Ermini L, Sallais J, Tagliaferro A, Todros T, Post M, and Caniggia I (2015) Aberrant TGFbeta Signalling Contributes to Dysregulation of Sphingolipid Metabolism in Intrauterine Growth Restriction. J Clin Endocrinol Metab 100, E986–996 [PubMed: 25942476]
37. Xu R, Wang K, Mileva I, Hannun YA, Obeid LM, and Mao C (2016) Alkaline ceramidase 2 and its bioactive product sphingosine are novel regulators of the DNA damage response. Oncotarget 7, 18440–18457 [PubMed: 26943039]
38. Xu R, Garcia-Barros M, Wen S, Li F, Lin CL, Hannun YA, Obeid LM, and Mao C (2018) Tumor suppressor p53 links ceramide metabolism to DNA damage response through alkaline ceramidase 2. Cell Death Differ 25, 841–856 [PubMed: 29229990]
39. Maceyka M, Sankala H, Hait NC, Le Stunff H, Liu H, Toman R, Collier C, Zhang M, Satin LS, Merrill AH Jr., Milstien S, and Spiegel S (2005) SphK1 and SphK2, sphingosine kinase isoenzymes with opposing functions in sphingolipid metabolism. J Biol Chem 280, 37118–37129. Epub 32005 Aug 37123. [PubMed: 16118219]
40. Mao C, and Obeid LM (2008) Ceramidases: regulators of cellular responses mediated by ceramide, sphingosine, and sphingosine-1-phosphate. Biochim Biophys Acta 1781, 424–434 [PubMed: 18619555]
41. Coant N, Sakamoto W, Mao C, and Hannun YA (2017) Ceramidases, roles in sphingolipid metabolism and in health and disease. Advances in biological regulation 63, 122–131 [PubMed: 27771292]
42. Xu R, Sun W, Jin J, Obeid LM, and Mao C (2010) Role of alkaline ceramidases in the generation of sphingosine and its phosphate in erythrocytes. FASEB J 24, 2507–2515 [PubMed: 20207939]
43. Li F, Xu R, Low BE, Lin CL, Garcia-Barros M, Schrandt J, Mileva I, Snider A, Luo CK, Jiang XC, Li MS, Hannun YA, Obeid LM, Wiles MV, and Mao C (2018) Alkaline ceramidase 2 is essential for the homeostasis of plasma sphingoid bases and their phosphates. Faseb j, fj201700445RR

44. Xu R, Jin J, Hu W, Sun W, Bielawski J, Szulc Z, Taha T, Obeid LM, and Mao C (2006) Golgi alkaline ceramidase regulates cell proliferation and survival by controlling levels of sphingosine and S1P. Faseb J 20, 1813–1825 [PubMed: 16940153]
45. Muller P, Janovjak H, Miserez A, and Dobbie Z (2002) Processing of Gene Expression Data Generated by Quantitative Real Time RT-PCR. BioTechniques 32, 1372–1379 [PubMed: 12074169]
46. Coan PM, Ferguson-Smith AC, and Burton GJ (2004) Developmental dynamics of the definitive mouse placenta assessed by stereology. Biol Reprod 70, 1806–1813 [PubMed: 14973263]
47. Wang K, Xu R, Schrandt J, Shah P, Gong YZ, Preston C, Wang L, Yi JK, Lin C-L, Sun W, Spyropoulos DD, Rhee S, Li M, Zhou J, Ge S, Zhang G, Snider AJ, Hannun YA, Obeid LM, and Mao C (2015) Alkaline Ceramidase 3 Deficiency Results in Purkinje Cell Degeneration and Cerebellar Ataxia Due to Dyshomeostasis of Sphingolipids in the Brain. PLoS Genetics 11, e1005591 [PubMed: 26474409]
48. Arroyo JA, and Winn VD (2008) Vasculogenesis and angiogenesis in the IUGR placenta. Semin Perinatol 32, 172–177 [PubMed: 18482617]
49. Xiong Y, Yang P, Proia RL, and Hla T (2014) Erythrocyte-derived sphingosine 1-phosphate is essential for vascular development. J Clin Invest 124, 4823–4828 [PubMed: 25250575]
50. Ben Shoham A, Malkinson G, Krief S, Shwartz Y, Ely Y, Ferrara N, Yaniv K, and Zelzer E (2012) S1P1 inhibits sprouting angiogenesis during vascular development. Development 139, 3859–3869 [PubMed: 22951644]
51. Kluk MJ, and Hla T (2002) Signaling of sphingosine-1-phosphate via the S1P/EDG-family of G-protein-coupled receptors. Biochim Biophys Acta 1582, 72–80. [PubMed: 12069812]

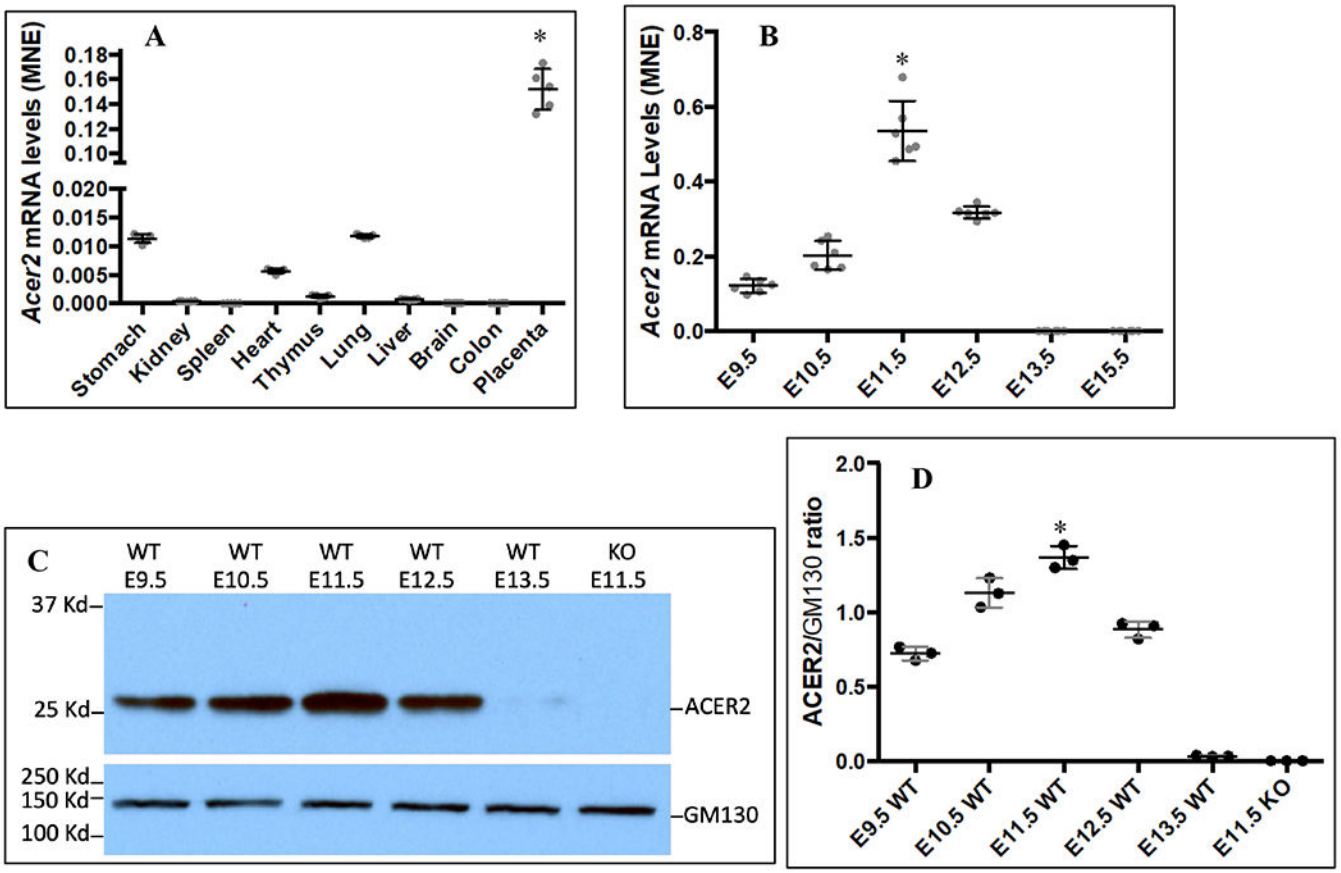

Figure 1. Acer2 is highly expressed in the placenta at developmental stages

A, total RNAs were extracted from placentas and major organs from pregnant mice (n=5) at 12.5 dpc and were subjected to qPCR analyses of *Acer2* mRNA levels; **B**, total RNAs were extracted from placentas (n=5, 1 per dam) of pregnant mice (n=5) at 9.5, 10.5, 11.5, 12.5, 13.5, or 15.5 dpc and subjected to qPCR analysis for *Acer2* mRNA levels as in A; **C and D**, total cell membranes were prepared from placentas (n=3 from 3 different pregnant mice at each time point) at different dpc and subjected to Western blot analyses using an antibody against ACER2 or GM130 (a Golgi complex marker as a sample-loading control). The image represents the results of 3 placentas (n=3) from 3 different pregnant mice. ACER2 and GM130 protein bands were revealed by the ECL kit (C) and the density ratio of the ACER2 vs GM130 band of each placenta was measured by the software Fiji (D). Data are presented as means ± SD and statistically analyzed by one-way ANOVA using the software Prims 8. *, $p<0.05$ vs other tissues (A) or time points (B and D).

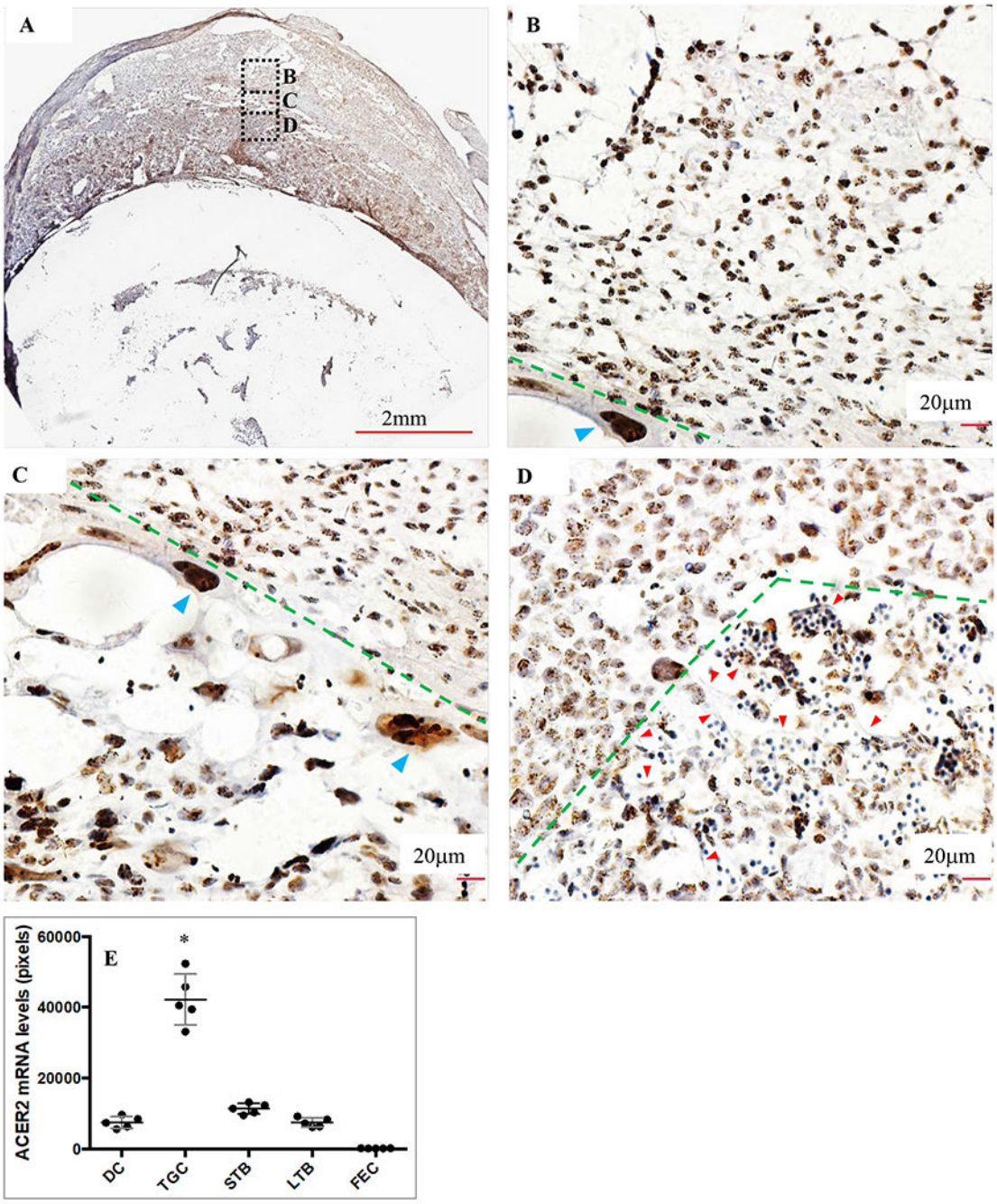

Figure 2. Acer2 is expressed in major cell types in the placenta

Tissue sections with a 7 μm thickness were prepared from paraffin-embedded WT placentas at E11.5 as described in Materials and Methods. The tissue sections close to the placental midline were subjected to *in situ* hybridization (ISH) using the *Acer2*-specific RNAscope probe. Brown colored dots represent *Acer2* mRNA molecules and nuclei were lightly counterstained blue with hematoxylin. A, an image of the placenta at a low microscopic magnification (50x); B, C, and D, the images were zoomed (200x) from the regions marked in A. B, the image showing decidual stromal cells (DC) above the green dotted line and P-

TGCs below the dotted line and pointed by blue arrowheads; C, the image showing DC above the dotted line, spongiotrophoblasts (STB) below the dotted line, and P-TGCs pointed by blue arrowheads; and D, the image showing STB above the dotted line and labyrinthine trophoblasts (LTB) below the dotted line and fetal endothelial cells (FEC) pointed by red arrowheads. The images in A-D represent the results of 5 placentas from 5 different dams. E, 5 sections from each of 5 placentas from 5 dams were imaged at 200x magnification and the images of 5 microscopic fields of view per section were obtained. Ten cells of each cell type were randomly selected from each microscope field of view and quantified for ISH signals (the pixels of brown colored dots) that correlate with the Acer2 mRNA levels using Fiji as described in Materials and Methods. Each dot in the graph represents the average of ISH signals (pixels per cell) from 250 cells of each cell type. Data are presented as means ± SD of 5 placentas and statistically analyzed by one-way ANOVA. * p <0.05 vs. indicated groups.

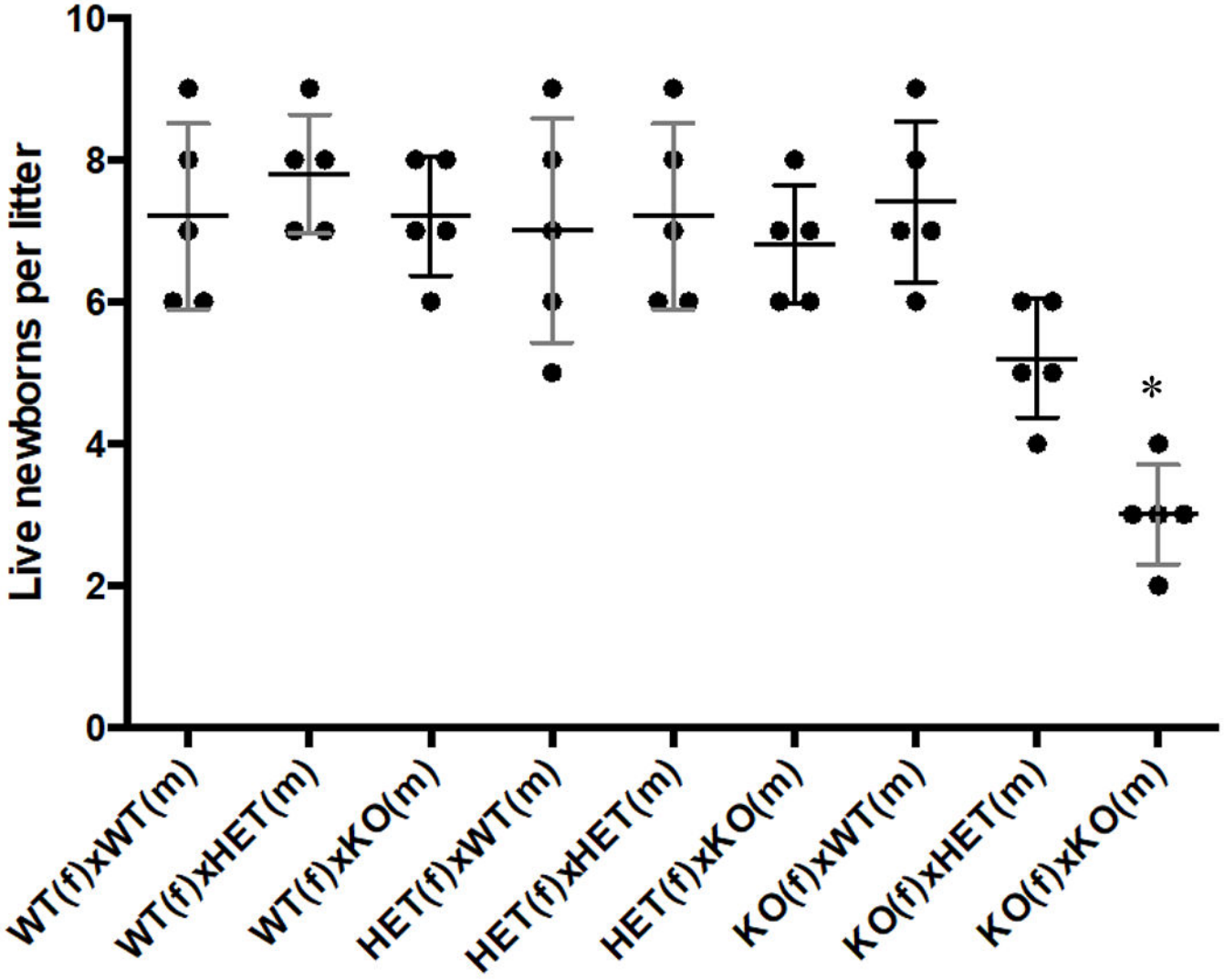

Figure 3. Acer2 deficiency in both the mother and embryo reduces litter size

Acer2$^{+/+}$, *Acer2*$^{+/-}$, or *Acer2*$^{-/-}$ females (n=5) were crossed with *Acer2*$^{+/+}$, *Acer2*$^{+/-}$, or *Acer2*$^{-/-}$ males, respectively, and the number of live newborns from 2nd and 3nd litters from each mating pair were recorded and the average litter size (the number of live newborns per litter) was computed. The 1st litters were skipped because some inexperienced mothers ate newborns right after parturition. WT, Acer2$^{+/+}$; KO, Acer2$^{-/-}$. Data are presented as means ± SD and statistically analyzed by one-way ANOVA. * p <0.05 vs. indicated groups.

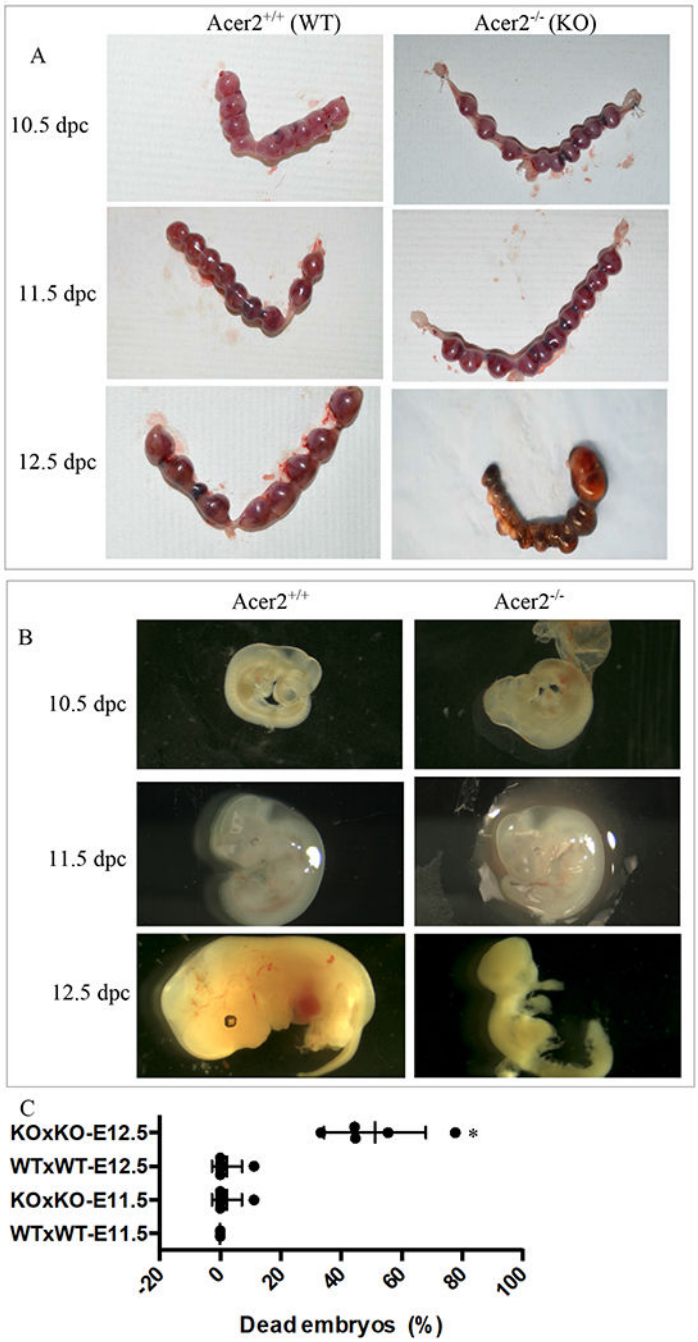

Figure 4. Acer2 deficiency causes death of embryos at E12.5

Necropsy was performed on pregnant *Acer2*$^{-/-}$ females (n=5) crossed with *Acer2*$^{+/+}$ males (n=5) or on pregnant *Acer2*$^{+/+}$ females (n=5) crossed with *Acer2*$^{+/+}$ males (n=5) at 10.5 dpc, 11.5 dpc, or 12.5 dpc. Uteri were dissected from pregnant mice (A), and embryos (B) were exposed from the uteri and the percentage of dead embryos in each dam was recorded (C). WT, Acer2$^{+/+}$; KO, Acer2$^{-/-}$. Data are presented as means ± SD and statistically analyzed by one-way ANOVA. * p <0.05 vs. indicated groups.

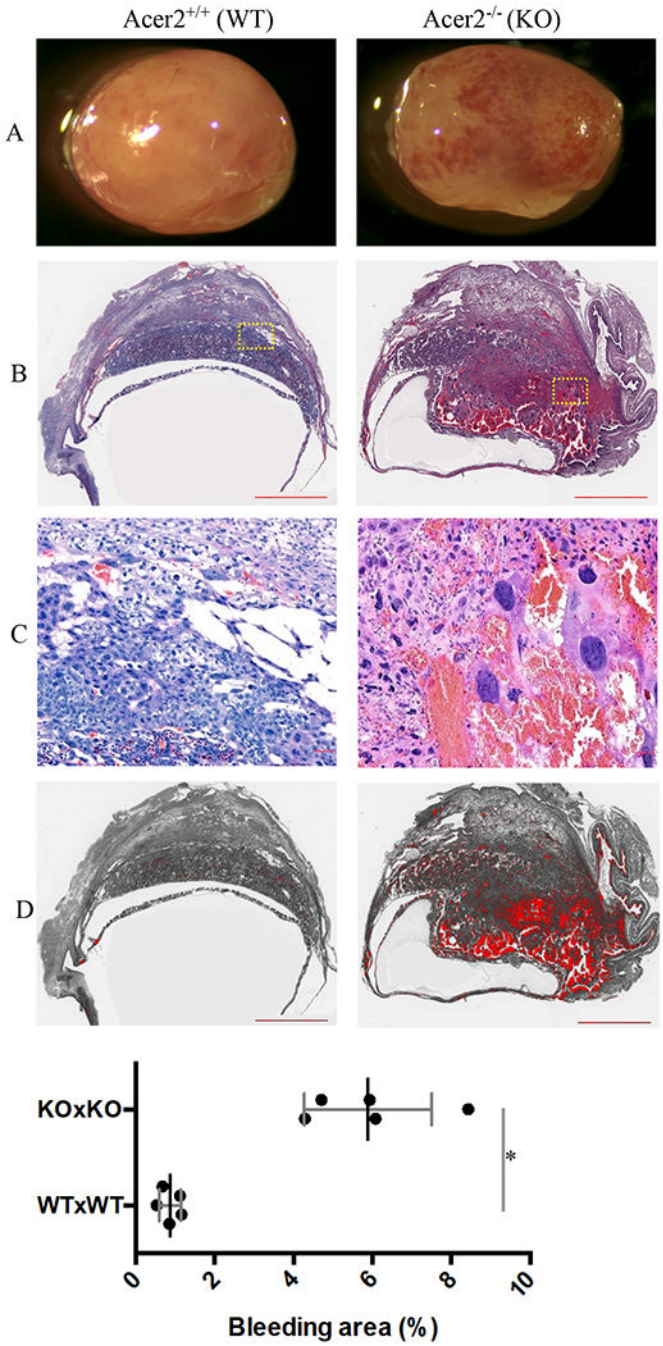

Figure 5. Acer2 deficiency causes hemorrhages of maternal blood in the junctional and labyrinthine zones

$Acer2^{+/+}$ (WT) and $Acer2^{-/-}$ E12.5 (KO) placentas at E12.5 (A) were processed into serial tissue sections as described in Materials and Methods. The tissue sections close to the placental midline were stained with a hematoxylin and eosin (H&E) solution and imaged under a microscope. The tissue sections (5 per placenta) were scanned under the microscope at 50x magnification (B). The areas in the rectangles in A were zoomed to reveal the bleeding areas (C). The images in A were converted to thresholded images (D) and total bleed areas were quantified with the software Fiji (E). The images represent the results of 5

placentas from 5 dams. The scale bars in B and D are 20 mm and those in C 20 μm. Data are presented as means ± SD and statistically analyzed by two-tailed Student's t-test. *, $p<0.05$ for the difference in bleed areas per placenta between Acer2$^{-/-}$ and Acer2$^{+/+}$ dams, which is considered significant.

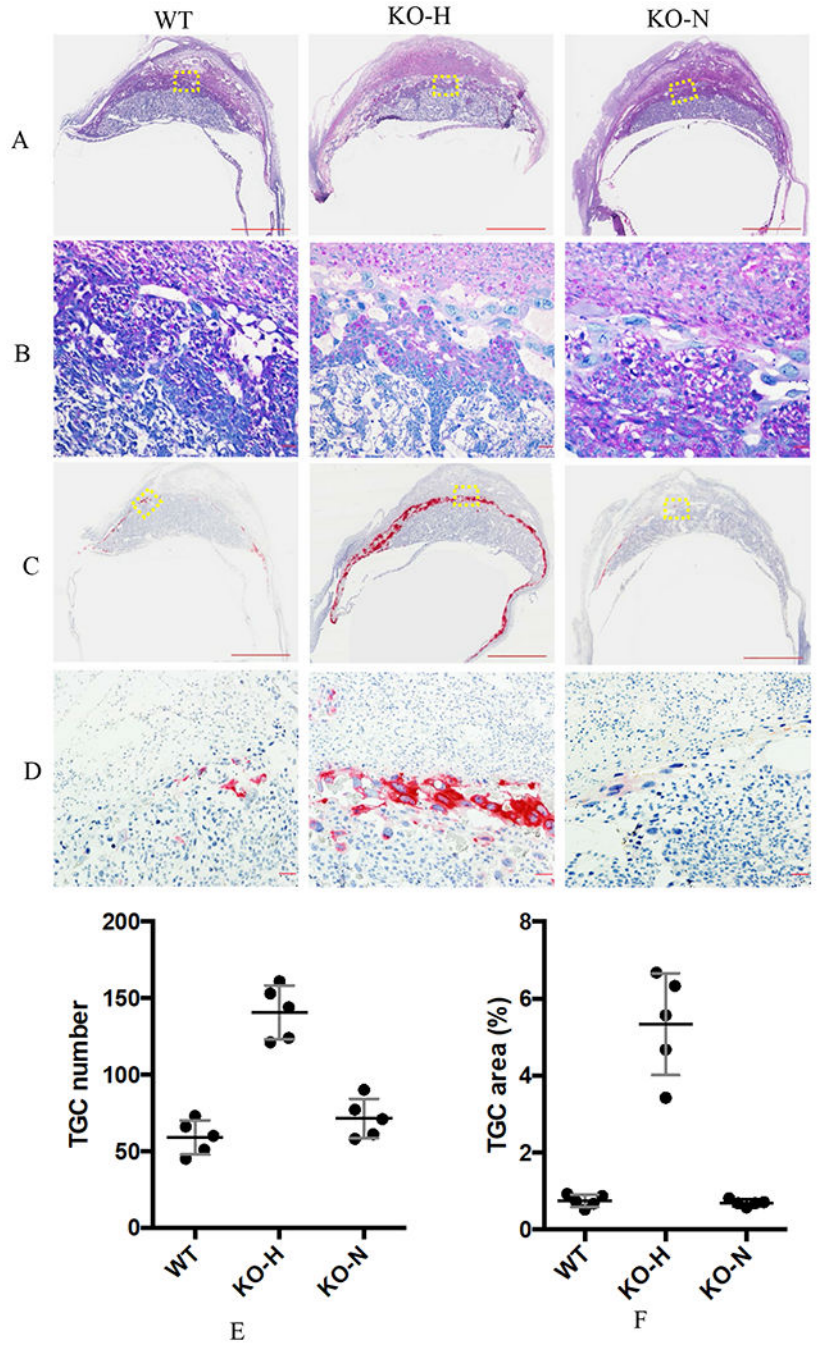

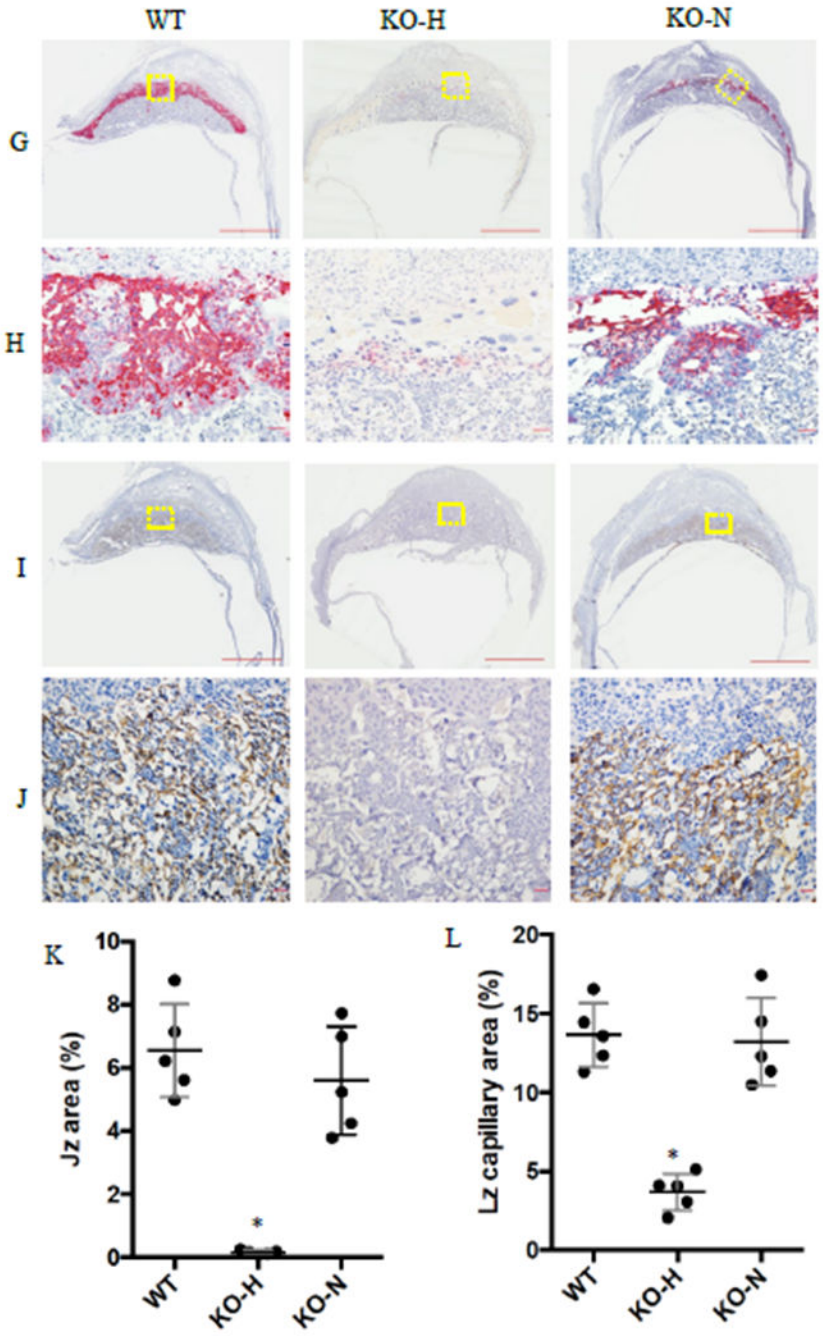

Figure 6. *Acer2* deficiency alters the placental architecture due to hemorrhages from the maternal vasculature

A-D, Tissue sections were prepared from E12.5 fetoplacental units from *Acer2*$^{-/-}$ or *Acer2*$^{+/+}$ dams (n=5) bred to *Acer2*$^{-/-}$ and *Acer2*$^{+/+}$ males, respectively, as described in Materials and Methods. The tissue sections close to the placental midline were stained with a PAS solution (A and B) or were subjected to ISH analysis using a RNAscope probe specific for the gene *Prl2c2 (C and D) or Tpbpa* (G and H), or were labeled with the biotinylated lectin IB4 (I and J). The areas stained with the RNAscope probes were shown in red and those stained with the IB4 lection in brown. The P-TGC numbers (E) and the areas

of the P-TGC layer (F) and Jz (K) and capillary areas (L) were quantified using the software Fiji. The images in B, D, H, and J were zoomed from the regions framed by the yellow rectangles in A, C, G, and I, respectively. Data are presented as means ± SD and statistically analyzed by one-way ANOVA. *, $p < 0.05$ vs. indicated group.

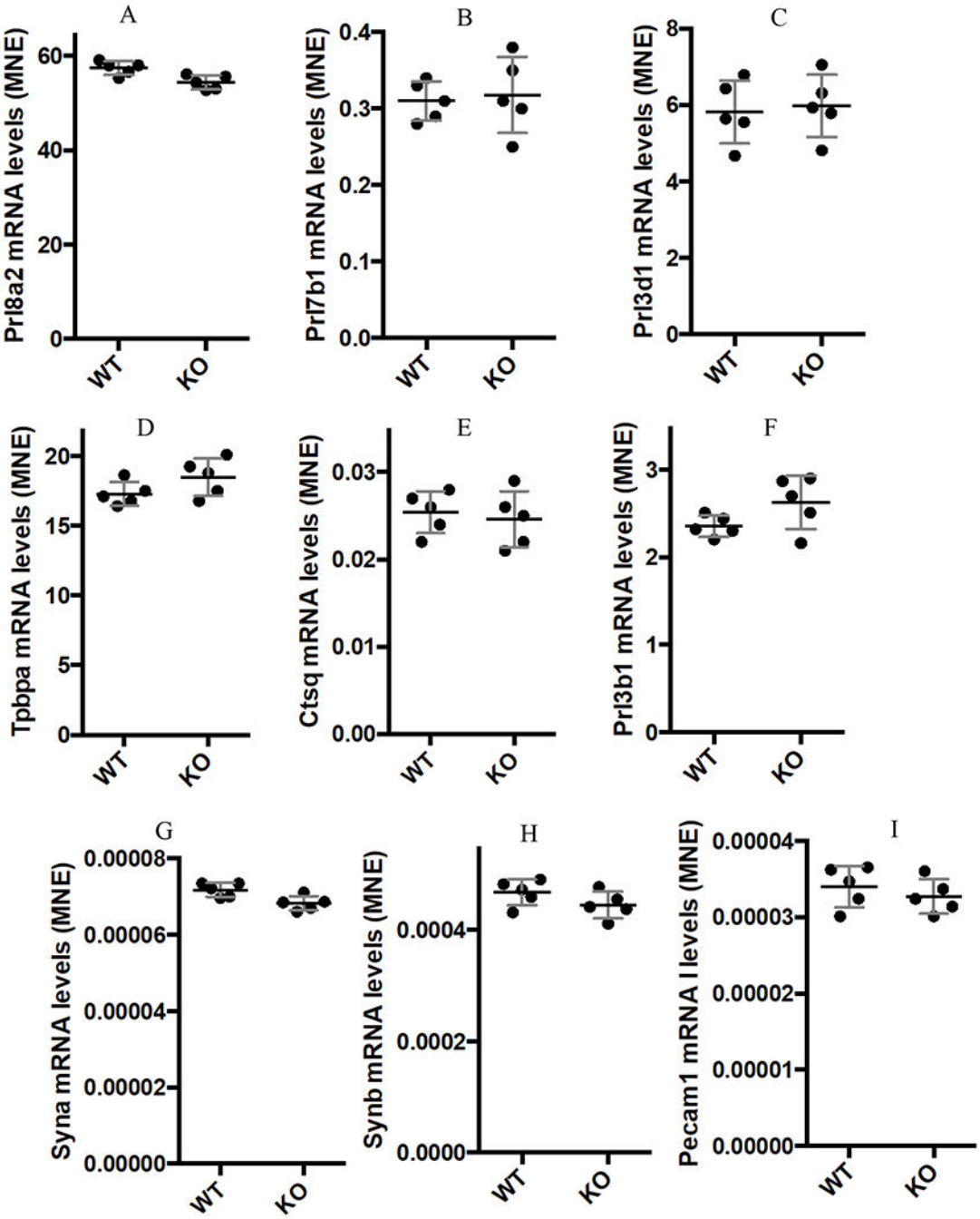

Figure 7. *Acer2* deficiency does not affect the expression of the differentiation markers of placental trophoblasts

E11.5 placentas (n=5, 1 per dam) were dissected from fetoplacental units from pregnant *Acer2*$^{+/+}$ and *Acer2*$^{-/-}$ females (n=5 per genotype) mated with *Acer2*$^{+/+}$ and *Acer2*$^{-/-}$ males, respectively. Total RNA was extracted from the placentas and subjected to qPCR analyses for mRNA levels of the indicated genes. Data are presented as means ± SD and statistically analyzed by two-tailed Student's t-test. The *p* value for the difference in the mRNA levels of each marker between the Acer2$^{+/+}$ and Acer2$^{-/-}$ placentas is greater than 0.05 and thereby considered insignificant.

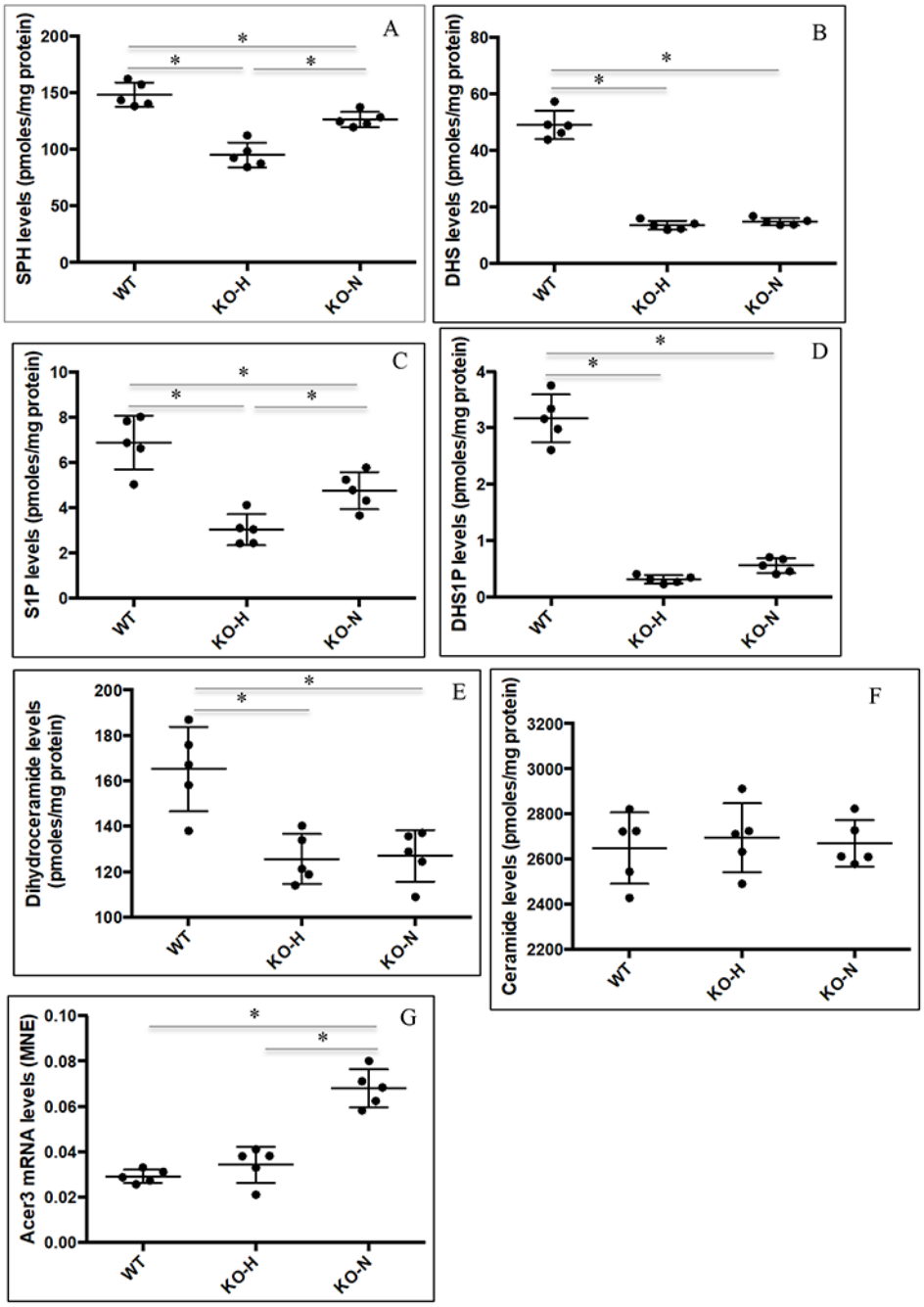

Figure 8. *Acer2* deficiency markedly reduces sphingoid bases, sphingoid base phosphates, and dihydroceramides in the placenta

Placentas (n=5, 1 per mother) were harvested from pregnant $Acer2^{-/-}$ mice (n=5) bred to $Acer2^{-/-}$ or from $Acer2^{+/+}$ mice (n=5) bred to $Acer2^{+/+}$ mice at E12.5. The harvested placentas (n=5 per genotype) were subjected to LC-MS/MS analyses of sphingosine (SPH) (A), dihydrosphingosine (DHS) (B), S1P (C), DHS1P (D), ceramides (E), and dihydroceramides (F). Acer3 mRNA levels were measured by qPCR. WT, placentas from $Acer2^{+/+}$ mice; KO-H, hemorrhagic plcentas from $Acer2^{-/-}$ mice; and KO-N, non-

hemorrhagic placentas from Acer2$^{-/-}$ mice. Data are presented as means ± SD and statistically analyzed by one-way ANOVA. *, $p<0.05$.

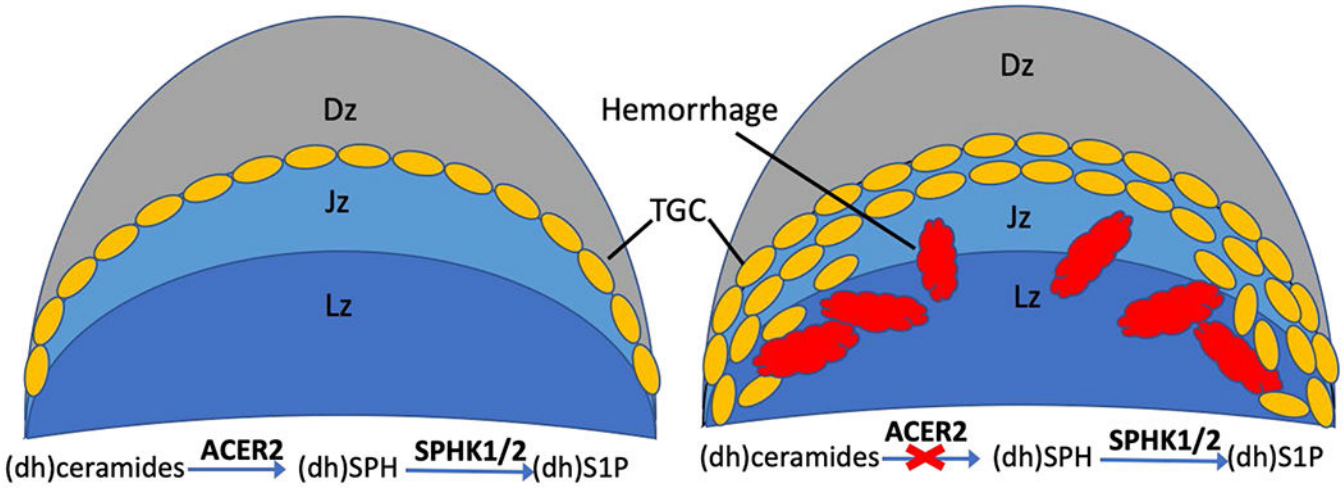

Figure 9. ACER2 regulates the homeostasis of sphingolipids and the integrity of the maternal vasculature and the placenta

ACER2 is highly expressed in most placental cell lineages if not all and its expression plays a key role in regulating the placental levels of sphingosine-1-phosphate (S1P) and dihydrosphingosine-1-phosphate (DHS1P) by controlling the generation of sphingosine (SPH) and dihydrosphingosine (DHS). Loss of ACER2 impairs the integrity of the maternal vasculature in the placenta, resulting in massive hemorrhages in the junction zone (Jz) and labyrinthine zone (Lz), an aberrant expansion of the trophoblast giant cell (TGC) layer, thereby fetal death.

Table 1

Primer pairs for qPCR

Gene	Forward primer	Reverse primer
Acer2	5’-GAGGACAACTACACTATCGTGCC-3’	5’-TAGATGCCGCTGTTGAAGCACG-3’
Acer3	5’-GATTCACTGAGGAACTTTCG-3’	5’-AGAGAAACTTCACTTTTGGC-3’
Ctsq	5’-GAGGCAGTAGTGGTCATCCC-3’	5’-CAGTACTTCTTCCTCCGGACT-3’
Pecam1	5’-CCAAAGCCAGTAGCATCATGGTC-3’	5’-GGATGGTGAAGTTGGCTACAGG-3’
Prl3b1	5’-CCAACGTGTGATTGTGGTGT-3’	5’-TGCCACCATGTGTTTCAGAG-3’
Prl3d1	5’-CCCCTGTGTCATACTGCTTCCA-3’	5’-TGAAAGACAACTCGGCACCTCA-3’
Prl7b1	5’-GGACACCAGTTTAGCAGCCTTT-3’	5’-CATTTCGCTAACACCTGATCCA-3’
Prl8a2	5’-GGGAGAAAGCTGCATCAATTCCT-3’	5’-GCTCTGAGAACCTCCTCATCACG-3’
Syna	5’-CTTTCCAAGGCTCTCTCGGACA-3’	5’-CTCAGCCACAATGAGGTCCAGA-3’
Synb	5’-CAAACACTGCCATACCTCTCCG-3’	5’-CACTGACATGGTAACAGGGTGG-3’
Tpbpa	5’-CCAGCACAGCTTTGGACATCA-3’	5’-AGCATCCAACTGCGCTTCA-3’
Actb	5’-TGTTACCAACTGGGACGACA-3	5’-GGGGTGTTGAAGGTCTCAAA-3’